15TH IEA HEAT PUMP CONFERENCE
MAY 26–29, 2026 | HOFBURG
VIENNA 2026
DECARBONISATION THROUGH INNOVATION

Design of a water-ammonia heat transformer with an ejector for low-pressure steam generation in extended operating range

Giovanni Vaghini[a*], Lorenzo Pistocchini[a], Tommaso Toppi[a]

[a]Energy Departement, Politecnico di Milano, Milano 20156, Italy

Abstract

Absorption heat transformers (AHTs) can contribute to the decarbonization of the industrial sector thanks to their capacity to upgrade intermediate-temperature waste heat to higher temperatures, suitable for industrial processes, while rejecting part of it to a lower temperature sink. Additionally, AHTs use much less electricity than heat pumps of the same heating capacity.

The European project ZIMBA aims to develop a single-stage water-ammonia AHT for steam production driven by waste heat. The system is designed to deliver 15 kW_{th} of steam at 1.3 bar(a) while working with a heat source at 80 °C and a heat sink at 20 °C. To extend the operability range, the integration of an ejector to decouple generator and condenser pressures is also introduced.

In this work, two cycle configurations are evaluated through numerical simulations under varying cold sink temperatures to assess system performance. The most promising configuration showed that at a sink temperature of 10 °C, the system achieves an electrical COP of 43.6, thermal COP of 0.47, and 15.1 kW_{th} of thermal output. At 35 °C, the identified cut-off condition, performance decreases significantly, with an electrical COP of 18.5, thermal COP of 0.38, and thermal output of 9.64 kW_{th}. This decline is mostly dependent on the increase in condensation pressure, which limits ammonia desorption in the generator.

These performances result from optimal concentration operation for each sink temperature; however, near cut-off, optimal concentration shifts significantly towards higher ammonia concentration, and without separate water and ammonia storage, hardly implementable in a heat transformer cycle, cut-off performance deteriorates further. But thanks to the ejector, at 35 °C, the most promising configuration achieves an electrical COP of 21.08, a thermal COP of 0.30, and 9.37 kW_{th} at a limited rise of ammonia concentration.

Keywords: Heat transformer; Absorption; Water-ammonia; Waste heat;

1. Introduction

The coming years call for a drastic transformation of the energy sector to achieve carbon neutrality by 2050 and limit global warming to below 1.5 °C by the end of the century. Industry plays a pivotal role in this transition, accounting in 2022 for around 25% of final energy consumption and 20% of total emissions in the European Union [1]. Most of this demand arises from process heating, which represents about 66% of industrial energy use, with 37% of it being required at temperatures below 200 °C. At the same time, the EU generates an estimated 2700 PJ/year of waste heat, corresponding to roughly 4% of its gross available energy [2], [3]. This context highlights the strong potential of heat pump technologies, which can upgrade waste heat to process-relevant temperature using either heat or electricity as the driving input, thereby enabling its reuse and reducing both energy consumption and CO_2 emissions. Nevertheless, in planning the transition toward a carbon-neutral society, careful consideration must be given to the pace and scale of industrial electrification, due to its significant impact on the electric grid.

Absorption heat transformers (AHTs) offer a suitable alternative for specific applications. Unlike vapor compression heat pumps, AHTs are thermally activated by the low-exergy waste heat available at intermediate

* *E-mail address:* giovanni.vaghini@polimi.it

temperature. The upgrade is accomplished through a distinctive thermodynamic cycle that raises the temperature of part of the heat input to the process level, while the remaining fraction is discharged to a low-temperature sink, with only negligible demand for mechanical work.

Although absorption heat transformers have been studied for several decades, the majority of realized systems rely on the LiBr–H_2O working pair, as shown by Cudok et al. [4], while only a limited number of studies and prototypes have explored water–ammonia AHTs. Compared to LiBr–H_2O, the NH_3–H_2O working pair offers favorable thermophysical properties, including lower corrosivity, absence of crystallization risk, and operation above atmospheric pressure, enabling more compact component design [5]. Despite these advantages, experimental investigations of NH_3–H_2O AHT performance has been limited. Among relevant works are those by Garone et al [6] and Liu et al. [7]. Garone et al. investigated driving temperatures between 60 and 64 °C with condenser temperatures ranging from 8 to 16 °C, reporting thermal COP values between 0.4 and 0.5. Liu et al., instead, studied a water–ammonia AHT driven at 85 °C for steam generation below 120 °C, reporting thermal COP values around 0.3 at absorber temperatures of approximately 105 °C under condenser temperatures between 27 and 32 °C. Among the advanced cycle concepts studies in absorption heat transformer reported by Rivera et al. [8] the only one investigating the integration of an ejector was performed by Sözen et al. [9]. In that work, an ejector was integrated into a single-effect absorption system to increase the pressure of the poor solution, resulting in improved cycle performance. However, the study primarily focused on cycle-level performance enhancement.

Building on these concepts, the European project ZIMBA was launched with the objective of developing a 15 kW_{th}, TRL-4 absorption heat transformer using water–ammonia as the working pair and commercially available components, such as ammonia-rated plate heat exchangers, valves, and welded stainless-steel piping. The system is designed for direct production of low-pressure steam, a valuable heating medium for the process heating in industries like food and beverage, textile, chemical and pulp and paper [10], [11]. The temperature levels for the development of this prototype were defined in line with the availability of waste heat and the industry requirements. The upgraded temperature has been identified at the saturation temperature of water at 1.3 bar(a) (∼107 °C), the intermediate temperature has been set at 80 °C, a typical waste heat temperature in industries like the food and beverage (Luberti et al. in [10]). Finally, the low-temperature heat sink is envisaged as an air-cooled condenser, resulting in a sink temperature variable with ambient air conditions in the range of 10–35 °C. This design objective removes the constraint of a fixed cold sink temperature, ensuring a broader operating range and a less dependency on the installation site characteristics.

This study presents the design process of a single-effect water–ammonia absorption heat transformer for the direct production of low-pressure steam. Two cycle layouts, referred as baseline configurations, are first considered, and their behaviours at nominal condition (i.e., 20 °C condenser water inlet temperature) are evaluated through numerical simulations. Subsequently, the most promising configuration is firstly analysed under varying cold sink temperature and later simulated with the addition of an ejector to assess its ability to extend the operating range at high cold-sink temperatures (i.e. 35 °C). Furthermore, the results show that, in addition to improving performance, the ejector stabilizes the average solution mass fraction, significantly reducing the reliance of the system on complex concentration control strategies that would otherwise be required to obtain similar performance without the ejector.

2. Methods

This section presents the approach adopted for the heat-transformer design. The design targets are first introduced, after which the two alternative cycle layouts considered for the baseline absorption heat transformer are described. Finally, the upgraded configuration with the ejector is presented.

2.1. Design objectives

The cycle layouts were developed to satisfy the following design targets:

- Pressure levels compliant with commercially available components.
- Volumetric flow rates of both refrigerant and solution pump in line with hermetic pump producers.
- The predicted temperatures from the simulations can be achieved with real heat exchangers without requiring impractically large surfaces.
- Thermal COP: $COP_{th} = \frac{|Q_{abs}|}{|Q_{gen}|+|Q_{eva}|} = 0.4$.
- Electrical COP: $COP_{el} = \frac{|Q_{abs}|}{|\mathrm{W}_{\mathrm{pmp,sol}}|+|W_{pmp,ref}|} = 40$.

- Upgraded heat capacity: $Q_{abs} = 15\ kW_{th}$.

The design process was supported by numerical simulations performed with the software STACY [12], a tool specifically designed for absorption cycles. STACY employs a modular approach, dividing the cycle into subsystems that represent the physical hardware components and automatically checks for the correct definition of the independent variables. The cycle is analysed under steady-state conditions, with pressure drops and heat losses neglected, and thermodynamic equilibrium assumed at the outlet of each component. This approach allows for a straightforward simulation of different cycle configurations. As a result, the main assumptions of the present approach are associated with the system-level formulation rather than with individual component models and are discussed in the following paragraph.

For a single-effect cycle, the internal model (i.e., excluding the external heat transfer processes with the sources and sinks) is typically defined by specifying the two pressure levels of the system, along with two additional mass-related conditions, such as the concentration or mass flow rate. The independent variables used to correctly formulate the internal problem in this study are listed in Table 1.

Table 1: Single effect heat transformer internal model inputs

Pressure conditions [13]	Low pressure	Subcooled condition at condenser outlet of 1 K
	High pressure	Subcooled condition at absorber outlet of 0.1 K
Mass conditions	Poor solution	Fixed mass flow rate of the solution pump
	Refrigerant	Fixed mass flow rate of the refrigerant pump

The imposed pressure conditions simulate the real behavior of the system as both absorber and condenser present self-adapting behavior. The presence of two-phase flow at the outlet (whether refrigerant at the condenser or rich solution at the absorber) will cause the pressure to rise, promoting further condensation or absorption, up to achieving a saturated or sub-cooled liquid condition. The conditions on the mass flow rates of the pumps, instead, do not realistically model the behaviour of the heat transformer as the flow rate are constrained by the throttling valve. However, this approach allows to retain numerical stability and easily identify operating conditions, while maintaining the possibility to replicate the simulated behaviour by properly regulating the real device.
Lastly, Table 2 presents the inlet temperatures and the temperature differences across each hydraulic circuit, with the condenser-water inlet temperature varied to define four distinct operating conditions.

Table 2: Single-effect heat transformer external model inputs

Component	Inlet temperature (°C)	Temperature difference across the hydraulic circuit
Generator	80	$\Delta T = 8\,°C$
Evaporator	80	$\Delta T = 8\,°C$
Condenser	10 – 20 – 30 - 35	$\Delta T = 5\,°C$
Absorber	106.5	$\Delta T = 0.5\,°C$

The temperature difference across the absorber corresponds only to the temperature increase required to bring the cooling water from the subcooled state to the evaporation temperature (∼107 °C). Water evaporation facilitates the distribution of the cooling stream across the plate heat exchanger channels, an essential aspect given the very low water mass flow rates required to produce 15 kW_{th} of heating capacity.
The outlet condition of the water is constrained by design to a two-phase state at 1.3 bar(a) to limit the high-pressure level of the cycle, which would otherwise be negatively affected by a superheated outlet condition.
The generated steam will then be subsequently separated from the liquid by means of a liquid–vapor separator installed downstream of the absorber.
Using the presented modeling framework and the defined design targets, two different cycle configurations were simulated.

2.2. System description – Option A: Single effect AHT with rectification section.

The first cycle analyzed, labelled as option A (Opt. A), is shown in Figure 1. It consists of a single effect configuration composed of an evaporator, a condenser, a generator, an absorber, two pumps to circulate the refrigerant and the poor solution, and an expansion valve. Additionally, it includes three internal heat recoveries implemented by the solution heat exchanger (SHX), the regenerative heat exchanger (RHE) and finally the internal heat recovery heat exchanger titled GEN2. The latter one is not commonly found in standard water ammonia heat transformers. Its main function is to ensure proper operation of the solution pump guaranteeing subcooled liquid at the suction line. To illustrate the operation of the system, the sequence of thermodynamic states of the working fluid along the cycle show in Figure 1 is described below.

A portion of intermediate-temperature heat drives ammonia desorption in the low-pressure generator, producing a poor solution (9) that is pumped to high pressure (11) and preheated in the SHX (12) before entering the absorber. In the absorber, this poor solution absorbs the high-pressure vapor coming from the evaporator (4), forming the rich solution (5) and releasing heat to the high-temperature sink. The rich solution then returns to the generator, passing through the SHX (6) and the expansion valve (7). Meanwhile, the desorbed refrigerant vapor (13P), after passing through the rectification section (13), enters the regenerative heat exchanger, where it transfers part of its energy to the pressurized liquid refrigerant (14). The vapor then condenses in the low-pressure condenser (1), after which the liquid refrigerant is pumped to high pressure (2), partially evaporates in the RHE through internal heat recovery (3), and is finally fully vaporized in the evaporator by the remaining heat at intermediate temperature. The rectification section' role is to increase the ammonia concentration of the generated vapor (13P) through partial condensation using the colder rich solution from the expansion valve.

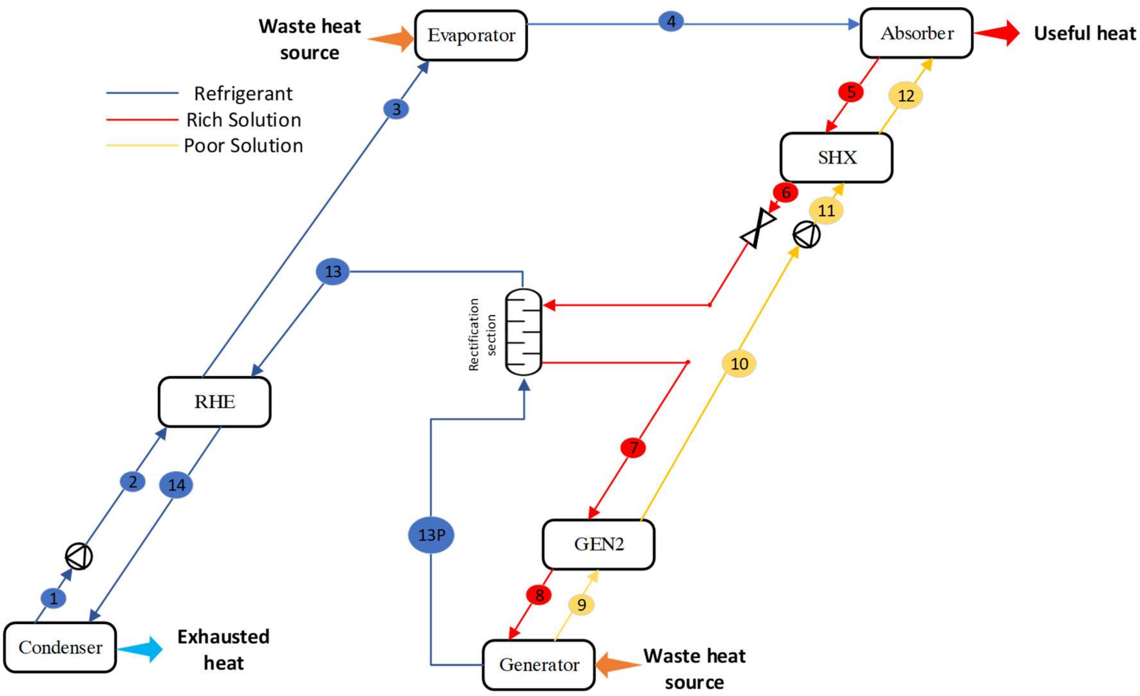

Figure 1: Option A - AHT cycle with rectification section

2.3. System description – Option B - Single effect AHT with additional internal heat recovery.

The second cycle, referred as option B (Opt. B) in this article, shown in Figure 2, remove the previously presented rectification section and add an internal heat recovery (labelled HEX in Figure 2) that exploit the sensible heat of the rich solution at the absorber outlet to increase the vapor title of the refrigerant stream. In the numerical model, both the generator and the absorber are represented as two plate heat exchangers connected in series. This modelling choice allows the required thermal length to be achieved while ensuring that each heat exchanger operates within a realistic range of size and performance, consistent with commercially available components.

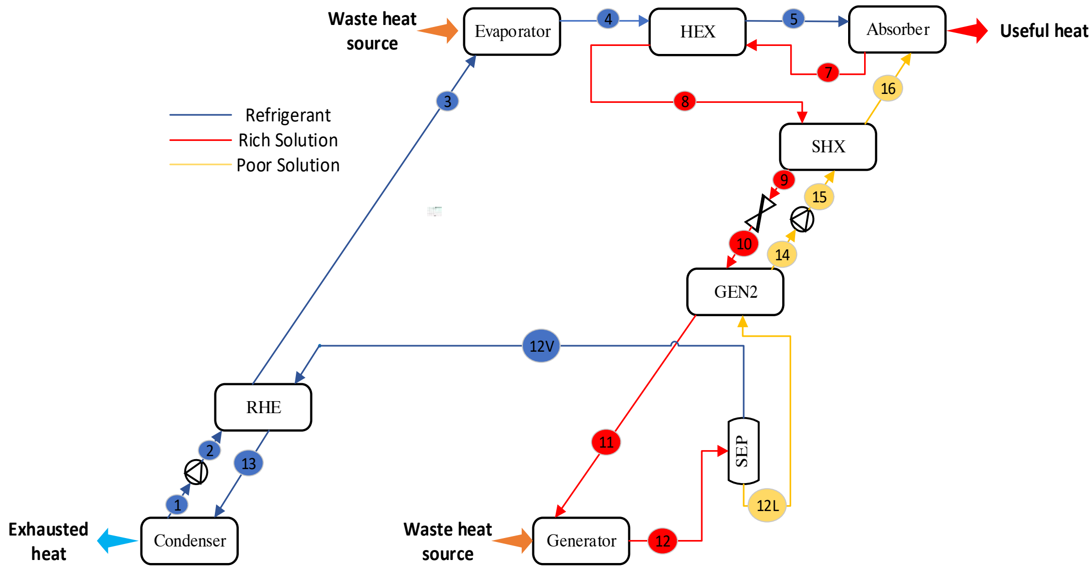

Figure 2: Option B - AHT cycle with additional internal heat recovery

2.3.1. System description – Option B U: Single effect AHT with additional internal heat recovery and ejector

In absorption heat transformers, after a certain condensation pressure, the inherent thermodynamic limitations of the single-effect cycle cause the electrical COP, thermal COP, and heating capacity to drop sharply, rendering the machine unsuitable for operation. This condition is referred to as the cut-off condition. To understand how to delay the onset of this condition the integration of an ejector was analyzed. This configuration, referred to as option B upgraded (Opt. B U), is shown in Figure 3. In the ejector, a fraction of the high-pressure, high-temperature refrigerant vapor (primary fluid) is used to entrain and compress the low-pressure vapor leaving the generator (secondary fluid). This process, known as thermal compression, decouples the generator pressure from the condenser pressure and mitigates the negative effect of elevated condenser inlet water temperatures.

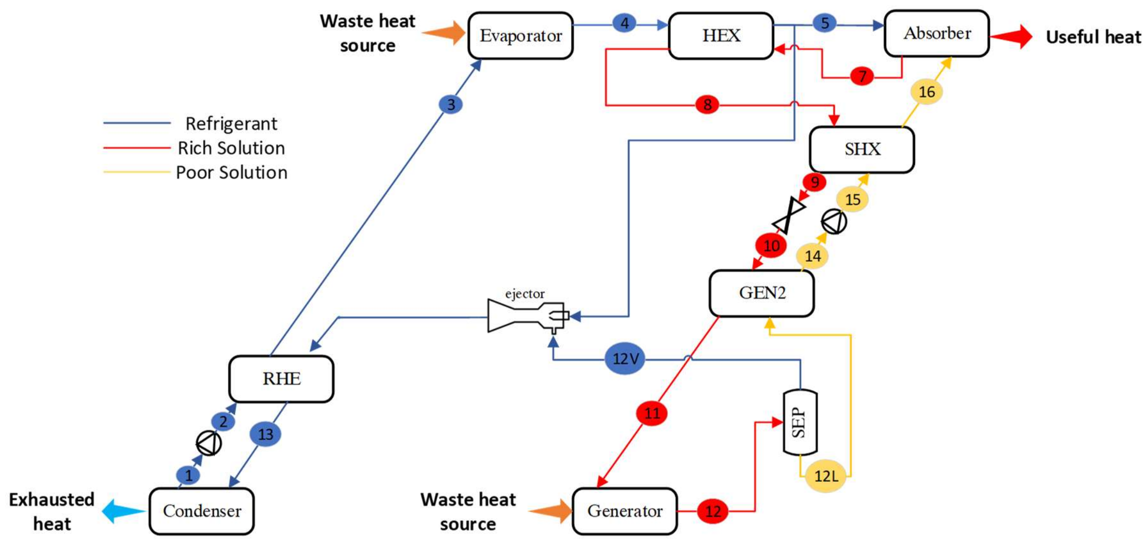

Figure 3: Option B U - AHT cycle with additional internal heat recovery and ejector

The ejector was modeled as a black box with two inlets and one outlet. The streams were assumed to behave as ideal gases composed of pure ammonia, and a second-law efficiency of 25% was imposed as suggested by Grazzini et al in [14]. The thermodynamic effect of the ejector was implemented in the STACY simulation environment by using 4 standard STACY components since the ejector subsystem is not available:

- Distributor : through the user defined split ratio the amount of high-pressure ammonia vapor diverted toward the ejector is set.
- Pump : artificially simulates the entrainment effect that the primary flow has on the secondary flow by increasing the pressure of the generated vapor with a negligible work input.
- Restrictor : decreases the pressure of the vapor coming from the evaporator to the outlet pressure of the generator, as in the converging duct of the ejector.
- A tee, where the 2 streams are mixed.

Introducing these 4 components requires the specification of an additional pressure condition as independent variable, which has been identified as the generator pressure. However, this introduces a circular dependency: the generator pressure must be set in STACY, but it also serves as an input for computing the outlet conditions of the ejector black box model (based on the assumed 25% efficiency).

To address this issue, an iterative procedure has been implemented. The process begins with an initial guess for the generator pressure, which is imposed in STACY. The simulation results are then passed to the simple numerical ejector model, where the second law efficiency is calculated. This loop continues, updating the generator pressure at each step, until the second-law efficiency corresponding to the conditions imposed in STACY converges to approximately 25%.

2.4. Modelling assumptions and limitations

The results presented in this study are influenced by a number of modelling assumptions that should be considered when interpreting the findings. In particular, the ejector is represented through a simplified thermodynamic model assuming ideal-gas behaviour for ammonia vapor and a fixed second-law efficiency of 25%, as suggested by Grazzini et al. [14]. While this value is consistent with literature data, variations in ejector efficiency due to geometry optimization, off-design operation, and real operation with a condensing ammonia–water mixture would directly affect the degree of pressure decoupling and, consequently, the achievable performance improvement. In addition, the analysis neglects pressure drops and heat losses in the system and assumes thermodynamic equilibrium at component outlets, which may lead to optimistic performance estimates under real operating conditions.

3. Results and discussion

In this section, a comparison between the operating points at nominal conditions for the two configurations is first presented. This is followed by a detailed analysis of the performance of the configuration labelled as Option B. Finally, the impact of the ejector on the performance of the most promising cycle configuration is discussed.

3.1. Comparison between Option A and Option B under nominal conditions.

The two cycle configurations analyzed differ by the ammonia concentration in the refrigerant branch. The water content in the stream has three major consequences:

1. Evaporation: A higher water content in the refrigerant stream increases the temperature glide, making complete evaporation more difficult and negatively affecting the absorption process.
2. Condensation: A higher water content in the refrigerant stream increases the bubble temperature of the working fluid, thereby favoring condensation at a given sink temperature.
3. The presence of water in the refrigerant stream for a fixed temperature of the sinks and source temperature lowers the high and low-pressures of the cycle.

The cycle behavior of option A, compared to the behavior of option B at same condenser water inlet temperature, is shown in the Dühring plot (PTx) in Figure 4. This type of representation can only display saturated liquid conditions. Depending on the specific component, the saturated liquid condition can occur within the heat exchanger. When this condition is met, it is represented in Figure 4 by the corresponding inlet and outlet states at the component interface (e.g., 2–3). Lastly, the letter M represent the adiabatic mixing point on top of the absorber.
Thanks to the rectification section in option A, high ammonia concentrations, above 99 %, are reached in the refrigerant branch. The simulation at 20 °C condenser water inlet temperature showed an electrical COP of 34.14, a thermal COP of 0.45, and a heat capacity of 15.02 kW_{th}.
The main technical limitation of option A is the high absorber pressure, which reaches 34 bar(a) at the design condition (20 °C water inlet temperature at the condenser). This pressure level is already close to the limits of ammonia-rated heat exchangers, suggesting that higher inlet temperatures would leave small safety margin for safe operation. Together with the added complexity of the rectification section and its limited impact on cycle performance, this configuration was considered suboptimal.

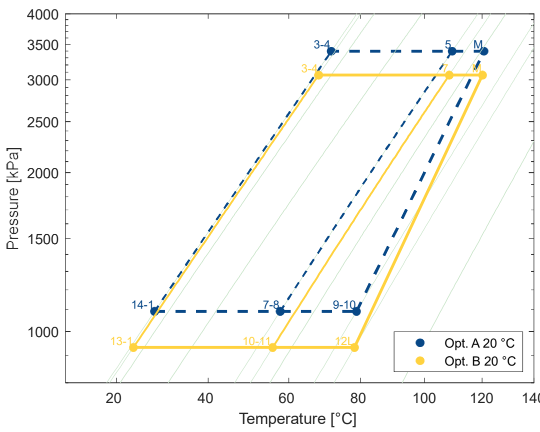

Figure 4: Dühring plot comparison of Option A and Option B

3.2. Analysis of option B - Single effect AHT with additional internal heat recovery.

The cycle operation points for condenser water inlet temperature from 10 to 35 °C are reported in Figure 5(a).

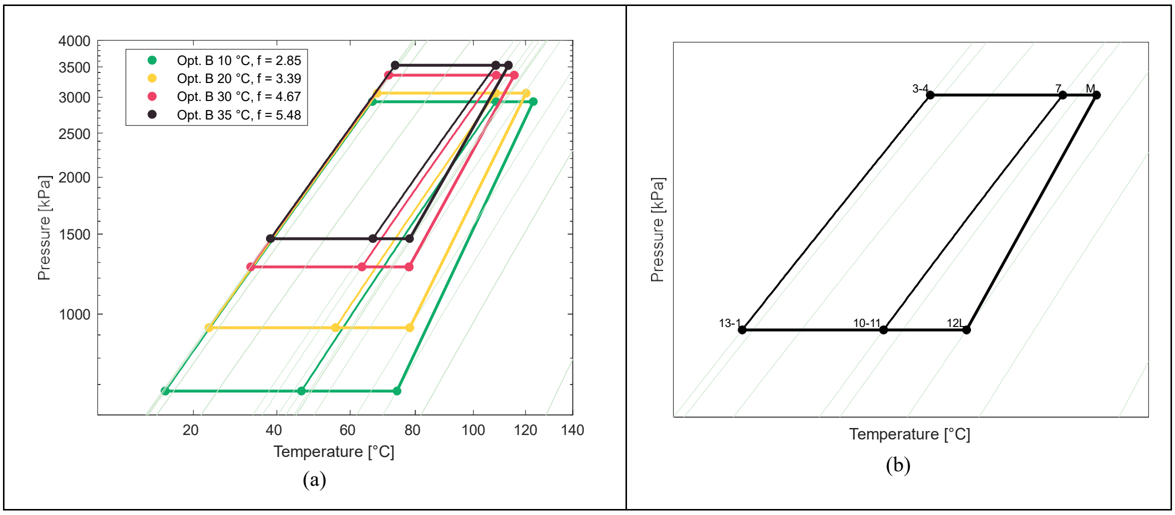

Figure 5: (a) Dühring plot comparison of option B under different condenser water inlet temperatures - (b) Representative operating point of option B.

The removal of the rectification section improves the overall pressure profile of the cycle, reducing the maximum pressure under the same boundary conditions. In the most challenging operating condition (35 °C coolant inlet temperature), the maximum pressure reaches 35 bar(a), which remains within the limits of commercially available ammonia-rated components.

The internal heat recovery section (identified as HEX in Figure 2) utilizes the sensible heat from the rich solution leaving the absorber to increase the refrigerant vapor quality allowing the system to achieve a thermal capacity of 15.1 kW_{th} at both the design point (20 °C) and the thermodynamically favorable 10 °C case, and still providing a heat capacity of 12.65 kW_{th} at 30 °C.

The observed decrease in thermal output results from the higher condenser water inlet temperature, which leads to an increase in the cycle's condensation pressure. This causes an increase in the concentration of the ammonia in both the rich and poor solutions, thereby reducing the heat released during the absorption process. To mitigate the inevitable decrease in performance, the circulation ratio (*f*), defined as the ratio between the mass flow rates of the poor solution and the refrigerant, is increased to sustain the absorption process.

This approach, can also be extended to a condenser coolant temperature of 35 °C, allowing the heat transformer to deliver 9.64 kW_{th} with a thermal COP of 0.38 and an electrical COP of 18.5.

The challenges in achieving such performance levels up to a coolant temperature of 35 °C primarily lie in managing the concentration variations required to reach these conditions. As shown in Figure 5, higher condenser temperatures demand higher ammonia concentrations in both the rich and poor solutions to reach the listed performances. Consequently, the concentration changes required to operate the system at optimal performance may necessitate a non-negligible transfer of working fluid between the active circulation loop and storage volumes. Such storage volumes would need to be placed upstream of both the solution and refrigerant pumps, where liquid inventories are available. The main difficulty of this approach arises from the absence of pure absorbent and pure refrigerant streams in a water–ammonia AHT.

Under unfavorable thermodynamic conditions, such as elevated condenser temperatures, optimal operation would require an increase in the water content of the solution branch. This would imply discharging poor solution from the solution-side storage to dilute the ammonia concentration in the solution loop. However, since the stored fluid is an ammonia–water mixture rather than pure water, the associated excess ammonia must be simultaneously accommodated in the refrigerant-side storage. This coupled charging and discharging of storage volumes significantly complicates control strategies and leads to an increase in the total ammonia inventory of the system. For these reasons, reducing reliance on large concentration variations and associated storage requirements is highly beneficial for practical prototype development.

Within the 10–30 °C range of condenser water inlet temperatures, concentration variations remain moderate and can likely be accommodated by the built in storage capacity of hermetic pumps and by proper flow control. However, at 35 °C, the required concentration adjustment, if not accommodated, would lead to a worsen in performance. To assess how the system behaves in the absence of working-fluid inventories, the cycle has been simulated limiting the variation in the average concentration between the rich and poor solutions from the 30 °C coolant condition to the 35 °C case.

In Figure 6 the operating point of the option B configuration at 35 °C of coolant temperature in the absence of storage capacity is shown compared to the 30 °C case.

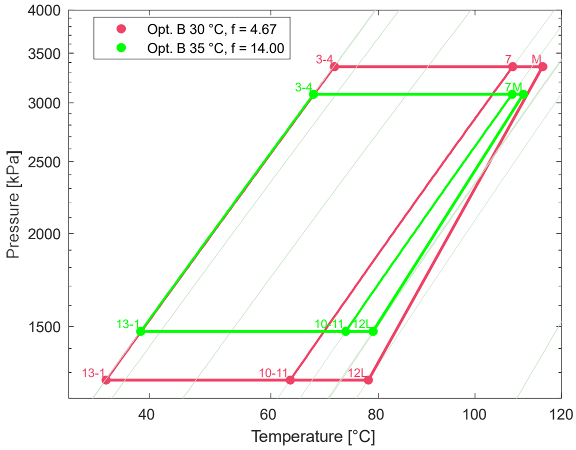

Figure 6: Duhring plot comparison of the simulation of the option B under varying coolant conditions with no concentration control.

The negative impacts on the performances are shown in Figure 7. The clear drop in both electrical COP and heat capacity underlines that at 35 °C the heat transformer in the absence of dedicated storage to allow the large concentration variation required to operate at the optimal condition would reach cut-off conditions.
The thermal COP is less affected since the load at the evaporator is highly reduced compared to the 30 °C case as the refrigerant mass flow rate is much smaller at the evaporator and generator reducing the heat required to drive evaporation and desorption.

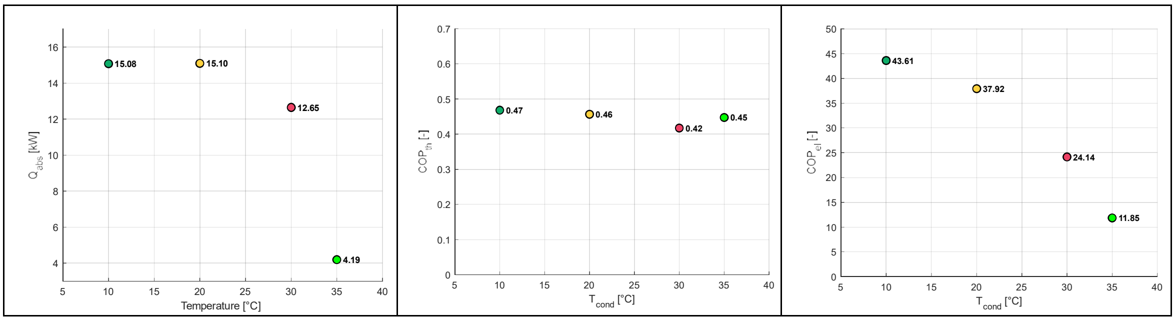

Figure 7: performances (heat delivered at the absorber, thermal COP, electrical COP) variation at different condenser water inlet temperatures.

3.3. Single effect absorption heat transformer with ejector

The previously presented simulation results highlight one key aspect in the design of a single effect absorption heat transformer: extending its operating range requires the decoupling of the condensation pressure and generator pressure. The integration of the ejector enables this decoupling. By entraining part of the low-pressure vapor leaving the generator using high-pressure refrigerant vapor, the ejector effectively reduces the generator operating pressure for a given condenser pressure. This alleviates the thermodynamic limitations associated with elevated sink temperatures, allowing ammonia desorption to occur under more favourable conditions and sustaining the absorption process. In addition, by decoupling generator and condenser pressures, the ejector reduces the need for large variations in solution concentration to maintain acceptable cycle operation at off-design conditions, thereby limiting the reliance on large working-fluid inventories and complex concentration control strategies. Figure 8 compares the relevant state points of option B in the absence of a concentration control strategy with those of the upgraded configuration (Opt. B U) at a coolant inlet temperature of 35 °C. The effect of the ejector is evident at point 12L (saturated liquid at the generator outlet), where the lower operating pressure in the upgraded AHT enables improved absorption performance. As a result, the system operates closer to optimal conditions while maintaining smaller variations in the average solution concentration, reducing the dependence on storage units and alleviating one of the major challenges associated with prototype development

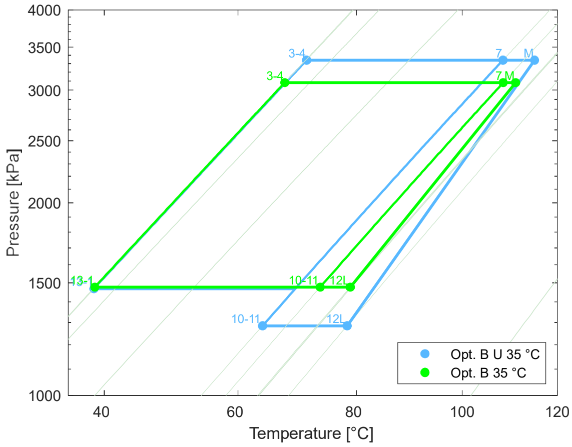

Figure 8: Dühring plot comparison between option B (Opt. B) and the upgraded configurations (Opt. B U) at a condenser water inlet temperature of 35 °C

Figure 9 illustrates the performance of the overall cycle across the complete operating spectrum. At 35 °C, the integration of the ejector yields a clear improvement in both the electrical COP and the heating capacity, compared to option B without dedicated storage vessels. The only downside in the ejector implementation is the reduction in the thermal COP. This decrease is caused by diversion of high-pressure, high-temperature vapor from the evaporator outlet to drive the ejector. This diverted stream increases the evaporator load while not contributing to the absorption process. The optimal split ratio, defined as the fraction of refrigerant vapor directed to the ejector, was set to 40% of the total ammonia vapor generated.

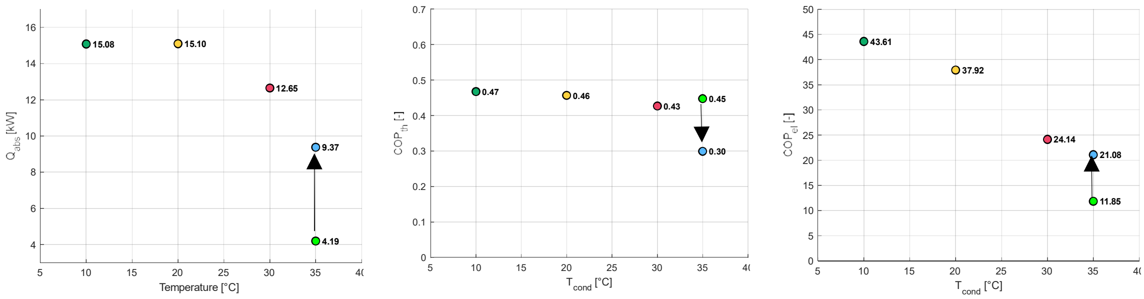

Figure 9: performances (heat delivered at the absorber, thermal COP, electrical COP) variation at different condenser water inlet temperatures.

4. Conclusions

In this study, two main AHT cycle configurations were simulated to evaluate which architecture best meets the requirements of the ZIMBA project. The results indicate that the configuration incorporating a rectification section (Option A) must be discarded due to excessive pressure levels (i.e., 34 bar(a)) observed already at design conditions. These pressures are already close to practical operating limits to most of standard components available on the market and raise safety concerns and will only worsen as condenser water inlet temperature increases.

The AHT baseline configuration, which operates with ammonia vapor of lower purity (Option B), maintains lower operating pressures while still achieving remarkable performance at nominal conditions. At the selected design point of 20 °C condenser water inlet temperature, the system delivered a thermal power output of 15.1 kW_{th}, a thermal COP of 0.46, and an electrical COP of 37.9.

Simulations also revealed performance degradation under off-design conditions. This degradation is accompanied by a significant variation in working fluid concentrations. Accommodating such fluctuations requires the implementation of storage vessels upstream of the pumps, introducing substantial technical and safety challenges in the system design.

To highlight the importance of a feasible concentration control strategy, a case without active control was simulated, revealing significantly worse results with a reduction in thermal power of 67% and in electrical

COP of 51% compared to the case at 30 °C coolant temperature.
To overcome both the off-design performance degradation and the complexity of managing large concentration swings, the introduction of an ejector was explored (Option B U). By decoupling the condenser and generator pressures, the ejector minimizes concentration variation in off-design conditions. This reduces the AHT system's reliance on storage tanks for concentration control, while improving both thermal output and electrical COP. The upgraded system can provide 9.37 kWth, and an electrical COP of 21.08 in the most degraded operating conditions.

Acknowledgment

This project has received funding from the European Union's Horizon Europe Research and Innovation programme under grant agreement No. 101146932.

References

[1] European Environment Agency, A c. di, *Trends and projections in Europe 2024*. Luxembourg: Publications Office, 2024. doi: 10.2800/7574066.
[2] D. Connolly *et al.*, *Heat Roadmap Europe 2: Second Pre-Study for the EU27*. Department of Development and Planning, Aalborg University, 2013.
[3] Eurostat, «Simplified energy balances». Eurostat, 2022. doi: 10.2908/NRG_BAL_S.
[4] F. Cudok *et al.*, «Absorption heat transformer - state-of-the-art of industrial applications», *Renewable and Sustainable Energy Reviews*, vol. 141, p. 110757, mag. 2021, doi: 10.1016/j.rser.2021.110757.
[5] E. Kurem e I. Horuz, «A comparison between ammonia-water and water-lithium bromide solutions in absorption heat transformers», *International Communications in Heat and Mass Transfer*, vol. 28, fasc. 3, pp. 427–438, apr. 2001, doi: 10.1016/S0735-1933(01)00247-0.
[6] S. Garone, T. Toppi, M. Guerra, e M. Motta, «A water-ammonia heat transformer to upgrade low-temperature waste heat», *Applied Thermal Engineering*, vol. 127, pp. 748–757, dic. 2017, doi: 10.1016/j.applthermaleng.2017.08.082.
[7] Z. Liu, D. Lu, S. Tao, R. Chen, e M. Gong, «Experimental study on using 85 °C low-grade heat to generate <120 °C steam by a temperature-distributed absorption heat transformer», *Energy*, vol. 299, p. 131491, lug. 2024, doi: 10.1016/j.energy.2024.131491.
[8] W. Rivera, R. Best, M. J. Cardoso, e R. J. Romero, «A review of absorption heat transformers», *Applied Thermal Engineering*, vol. 91, pp. 654–670, dic. 2015, doi: 10.1016/j.applthermaleng.2015.08.021.
[9] A. Sözen e H. S. Yücesu, «Performance improvement of absorption heat transformer», *Renewable Energy*, vol. 32, fasc. 2, pp. 267–284, feb. 2007, doi: 10.1016/j.renene.2006.01.017.
[10] M. Luberti, R. Gowans, P. Finn, e G. Santori, «An estimate of the ultralow waste heat available in the European Union», *Energy*, vol. 238, p. 121967, gen. 2022, doi: 10.1016/j.energy.2021.121967.
[11] A. Marina, S. Spoelstra, H. A. Zondag, e A. K. Wemmers, «An estimation of the European industrial heat pump market potential», *Renewable and Sustainable Energy Reviews*, vol. 139, p. 110545, apr. 2021, doi: 10.1016/j.rser.2020.110545.
[12] M. Aprile, T. Toppi, S. Garone, e M. Motta, «STACY–A mathematical modelling framework for steady-state simulation of absorption cycles», *International Journal of Refrigeration*, vol. 88, pp. 129–140, apr. 2018, doi: 10.1016/j.ijrefrig.2017.12.019.
[13] N. Demesa, J. A. Hernández, J. Siqueiros, J. C. Garcia, e A. Huicochea, «Improvement of the performance of an absorption heat transformer through a single effect process to obtain freshwater», *Applied Thermal Engineering*, vol. 78, pp. 162–171, mar. 2015, doi: 10.1016/j.applthermaleng.2014.12.039.
[14] G. Grazzini, A. Milazzo, e F. Mazzelli, «Ejector CFD Modeling», in *Ejectors for Efficient Refrigeration: Design, Applications and Computational Fluid Dynamics*, G. Grazzini, A. Milazzo, e F. Mazzelli, A c. di, Cham: Springer International Publishing, 2018, pp. 117–150. doi: 10.1007/978-3-319-75244-0_4.